CSIRO PUBLISHING

International Journal of Wildland Fire
http://dx.doi.org/10.1071/WF16080

Research Note

Chaparral growth-ring analysis as an indicator of stand biomass development

Kellie A. Uyeda[A,B,E], *Douglas A. Stow*[A], *John F. O'Leary*[A], *Christina Tague*[C] *and Philip J. Riggan*[D]

[A]Department of Geography, San Diego State University, 5500 Campanile Drive, San Diego, CA 92182-4493, USA.
[B]Department of Geography, 1832 Ellison Hall, University of California, Santa Barbara, CA 93106-4060, USA.
[C]Bren School of Environmental Science and Management, University of California, 2400 Bren Hall, Santa Barbara, CA 93106, USA.
[D]Pacific Southwest Research Station, USDA Forest Service, 4955 Canyon Crest Drive, Riverside, CA 92507, USA.
[E]Corresponding author. Email: kellie.uyeda@gmail.com

Abstract. Chaparral wildfires typically create even-aged stands of vegetation that grow quickly in the first 2 decades following a fire. Patterns of this growth are important for understanding ecosystem productivity and re-establishment success, but are logistically challenging to measure over long time periods. We tested the utility of a novel method of using shrub growth rings to estimate stand-level biomass accumulation at an annual time scale in southern California chaparral. We examined how temporal variation in precipitation and spatial variation in solar irradiation influence that accumulation. Using field measurements and a relationship between stem basal area and aboveground biomass, we estimated current biomass levels in an 11-year-old chaparral stand, and used growth-ring diameters to estimate growth in each year from age 4 to 11 years. We found that annual growth as measured by shrub growth rings tracked closely with patterns of annual precipitation, but not with time since fire. Solar irradiation was not found to be a significant covariate with total biomass by plot, possibly due to sampling area limitations. The close relationship of annual biomass accumulation with annual precipitation indicates that shrub growth-ring measurements can provide a useful metric of stand-level recovery.

Additional keywords: basal area increment, biomass accumulation, California, *Ceanothus*, dendrochronology, fire ecology, fuel, productivity, San Dimas Experimental Forest, wildfire.

Received 9 December 2015, accepted 24 May 2016, published online 23 June 2016

Introduction

Wildfires are a common disturbance in chaparral ecosystems and typically consume nearly all aboveground biomass other than the largest live woody stems. Subsequent regrowth – by sprouting from underground lignotubers or seedling establishment – accumulates woody biomass, which sequesters carbon, represents fuel available for future fires and is closely related to future ecological fire effects (Riggan *et al.* 1988). Rates and spatial patterns of regrowth are likely affected by both water availability – which can be spatially and temporally variable – and structural limitations in the development of woody stems, which may provide a predictable pattern to biomass accumulation with time. It is important to understand biomass accumulation because of its link to future wildfires, especially in an era of global climate change, which in California is expected to result in higher temperatures and altered precipitation regimes (Cayan *et al.* 2008; Pierce *et al.* 2013). These climate changes might directly affect fuel temperature and moisture at the time of burning, but their impact on productivity and fuel load is likely paramount in their effect on fires. We will be able to understand such linkages of climate, structural growth and fire only through detailed measurement and modelling of the regrowth.

Chaparral productivity has been measured in the field for a limited number of years and locations (e.g. Schlesinger and Gill 1980; Black 1987; Pasquini and Vourlitis 2010) and by using satellite-based vegetation metrics for a time-span of up to a decade (Hope *et al.* 2007; Kinoshita and Hogue 2011), but tracking productivity in the field over a decade is logistically challenging. In the present study, we test a novel method for measuring stand-level biomass accumulation at an annual time scale based on changes in shrub growth rings, and examine how temporal variation in precipitation and terrain-related site characteristics co-vary with biomass accumulation patterns in a high-productivity chaparral environment.

Journal compilation © IAWF 2016

Chaparral species that only are established by seed germination immediately following a fire (obligate seeders) produce annual growth rings that can be interpreted fairly easily because they form even-aged stands and for several years are especially sensitive to seasonal water availability due to their shallow roots (Keeley 1993). With the assumption that the diameter of each growth ring corresponds to the diameter of the shrub at the end of that growing season, obligate seeder species provide an opportunity to measure annual increases in shrub biomass.

Whereas previous studies have used chaparral growth rings to determine stand or shrub age (Stohlgren *et al.* 1984; Keeley 1993; Zammit and Zedler 1993; Duren and Muir 2010; Smith 2016), shrub response to precipitation (Coale *et al.* 2011) and biomass accumulation at a time scale of every 7 years (Riggan *et al.* 1988), research relating growth rings to biomass at an annual scale is more common for (non-chaparral) trees (e.g. Clark *et al.* 2001; Bouriaud *et al.* 2005).

We address the following research questions within the context of understanding patterns of post-fire biomass accumulation in shrublands:

1. How effective are measurements of shrub growth-ring increments as a metric of biomass accumulation?
2. How does biomass accumulation of recovering shrubs, measured as the change in growth-ring width, vary with differences in annual precipitation and time since fire?
3. How do spatial patterns of shrub biomass vary with solar irradiation levels estimated from digital elevation data?

Methods

Study site

The San Dimas Experimental Forest (SDEF) is a research site managed by the USDA Forest Service located in the San Gabriel Mountains in Los Angeles County, CA, USA. Vegetation there is predominantly mixed chaparral, with limited areas of coastal sage scrub, oak woodland and mixed conifers. The obligate-seeding species *Ceanothus crassifolius* (all nomenclature follows Baldwin *et al.* (2012)) is common on south-facing slopes, and *Ceanothus oliganthus*, another obligate seeder, is common on north-facing slopes. The entire study site burned in 2002. This area experiences a Mediterranean-type climate, with hot, dry summers and cool, wet winters. Average precipitation for the area is ~720 mm (http://www.prism.oregonstate.edu/, accessed 4 April 2014). Reference data are available from a previous study (Riggan *et al.* 1988) that estimated biomass accumulation for stands within this site at ages of 7 and 14 years using growth-ring reconstruction for 21-year-old shrubs based on regressions for biomass components as a function of basal area at each of these ages.

Field methods

Field plots were located within two 6.25-ha areas (250 by 250 m) within 500 m of one another. We established three randomly located, replicate plots, each 16 m^2 (4×4 m), stratified by aspect (north, south, east, west), in each of the two 6.25-ha study areas. This design resulted in 12 plots per study area and a total of 24 plots for the entire study area (Fig. 1). All plot sampling took place in the autumn of 2013 at a vegetation age of 11 years. The sampling methods were similar to those used in a previous study of California chaparral (Uyeda *et al.* 2016).

We measured stems from all shrubs present in each plot to estimate aboveground biomass. Species-specific regression equations relating stem basal area to dry biomass were based on stems sampled during the 2013 field campaign and during an earlier field campaign in the autumn of 2011. Full details on field methods are provided in the online supplementary material.

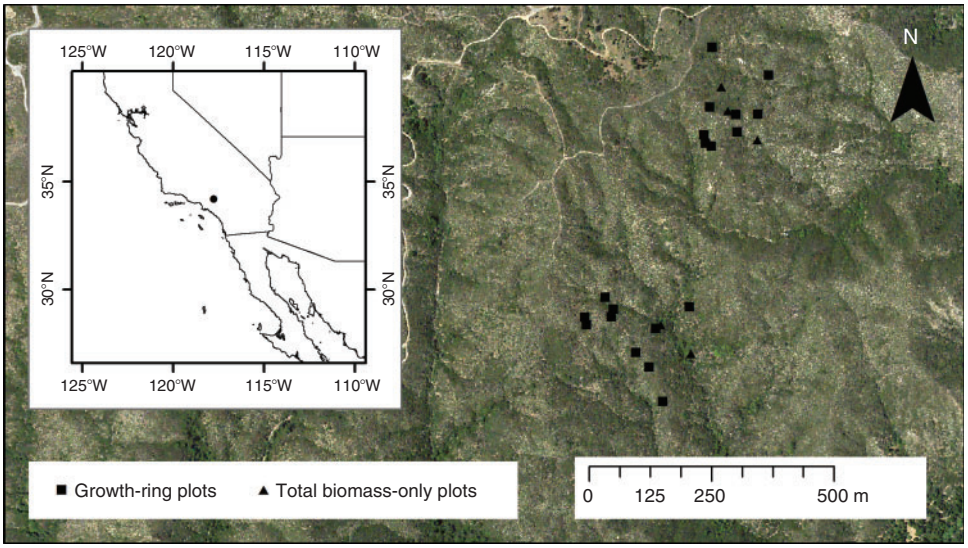

Fig. 1. Location of San Dimas Experimental Forest (SDEF) and individual plot locations. Total biomass was measured at all 24 field plots, and growth rings were successfully processed at 19 of the plots. Background imagery is from the National Agricultural Imagery Program, acquired in 2012.

Growth-ring processing

Stem cross-sections from five randomly selected *Ceanothus* spp. (*C. crassifolius* and *C. oliganthus*) shrubs from each study plot were harvested in the field at a height of 10 cm. When a shrub had more than one stem present at 10 cm, the largest stem was used. The stem cross-sections were sanded with progressively finer sandpaper up to 400 grit and photographed using a flat platform and stationary camera. We then measured the growth-ring diameters along the maximum and minimum axis of each cross-section using *ImageJ* software (version 1.44, http://imagej.nih.gov/ij/, accessed 8 January 2014). An example stem cross-section is shown in Fig. S1 in the online supplementary material.

We calculated the basal area for each year of growth using the mean of the maximum and minimum diameter measurements. Each year of growth was then converted to a percentage of the total area (representing growth at the end of 2013), and the mean percentage increment in basal area was calculated for each plot. We assumed that the bark width was a constant ratio of the total stem diameter (Husch *et al.* 2003) and therefore used the inside bark measurements to calculate the percentage increment values.

We applied the average plot-level percentage increment to all live stems measured in each plot to estimate basal areas for each year of post-fire growth. The annual plot-level biomass was then calculated for each year post-fire using these estimated basal areas and the species-specific regression equations described earlier. We did not attempt to evaluate biomass trends of dead stems because it was difficult to determine the age at which stems had died. Although dendrochronological studies typically use standardised growth-ring widths to account for the decline in ring width with age (Fritts and Swetnam 1989), in the current study, we used total area values because we related stem area directly to plot-level biomass increment.

Analysis of site characteristics

We estimated annual solar irradiation for each plot in order to explore spatial patterns related to energy and water balance. Sites with low irradiation levels are typically more mesic than sites with high irradiation due to lower evapotranspiration rates (Röder *et al.* 2008), with lower biomass typically associated with sites with higher irradiation (Yool *et al.* 1985). We calculated the annual irradiation at the centre of each plot using a lidar-based digital elevation model (DEM), resampled to 5 m, as input into the hemispherical viewshed algorithm implemented in *ArcGIS* software (Rich *et al.* 1994). We also used the DEM to calculate the actual slope aspect of each plot, as slight errors in plot placement sometimes resulted in actual plot aspects that did not match the originally planned aspect. We then grouped the plots into three categories based on aspect: north-east to north-west, south-east to south-west, and directly east- or west-facing.

To provide an additional assessment of field-based estimates of biomass, we calculated the average Normalized Difference Vegetation Index (NDVI) for each plot using colour infrared imagery with a spatial resolution of 1 m. The imagery was collected in May 2012 as part of the National Agriculture Imagery Program. NDVI was calculated as the difference of plot-averaged digital number values for the near-infrared and red wavebands divided by the sum of those values for each plot. NDVI is widely used in remote-sensing studies as a metric of vegetation greenness and is often well correlated with biophysical variables such as green biomass (Jensen 2007). Examining the plot-averaged NDVI for a date near the end of the study period allowed us to compare another metric of vegetation abundance (independently of the field-measured biomass) with the annual solar irradiation.

Data analysis

We examined the relationship between annual precipitation, year since fire and average annual biomass growth by calculating Pearson's product correlation coefficient (r) for each pair of variables ($n = 7$). Precipitation data were obtained from the Parameter-elevation Regressions on Independent Slopes Model (PRISM) climate group (http://www.prism.oregonstate.edu/, accessed 4 April 2014) and summed by the hydrologic year (the 12-month period starting 1 October of each year, designated by the calendar year in which it ends).

We performed three linear regression analyses: total biomass as a function of modelled irradiation ($n = 24$), total biomass as a function of NDVI ($n = 24$), and NDVI as a function of modelled irradiation ($n = 24$). We examined the coefficient of determination (R^2) for each regression. All statistical analyses were conducted using the *R* statistical software package.

Results

Plot biomass

Regression models of biomass as a function of basal area for the five chaparral species are presented in Fig. S2. The R^2 values for the live biomass equations range from 0.79 to 0.98, whereas the values for dead biomass are lower and range from 0.29 to 0.89 (Table S1).

The shrubs density found on each plot ranged from 0.8 to 4.5 individuals m^{-2} (Table S2). The average biomass of live shrubs, including any attached dead material, at the time of field sampling (11 years old) was 2.6 kg m^{-2}, with a range of 1.0–6.7 kg m^{-2} (Table S3). The biomass of dead material on live shrubs typically was less than 5% of total biomass, although it was occasionally as high as 10%. *Ceanothus crassifolius* occurred in high abundance on most plots, and *Adenostoma fasciculatum* and *Salvia mellifera* were also commonly present.

Growth rings

Of the 24 field plots, five were removed from analysis because there were fewer than three stem cross-sections per plot of suitable quality (Table S2). We found that it was difficult to clearly determine ring position in stems smaller than ~1 cm. In addition, some shrubs had heart rot or insect damage, which obscured the centre rings, and in other shrubs, the smallest centre rings were difficult to differentiate. In order to make use of the stems that lacked rings from the earliest years of post-fire recovery while maintaining a consistent number of measurements per year in each plot, we started the analysis at the fourth year of post-fire recovery (the 2005–06 growing season). The diameters of each stem used in this analysis are shown in Table S4.

The percentage of total stem area in each year is shown for each of the final 19 plots in Fig. S3*a*. The difference between

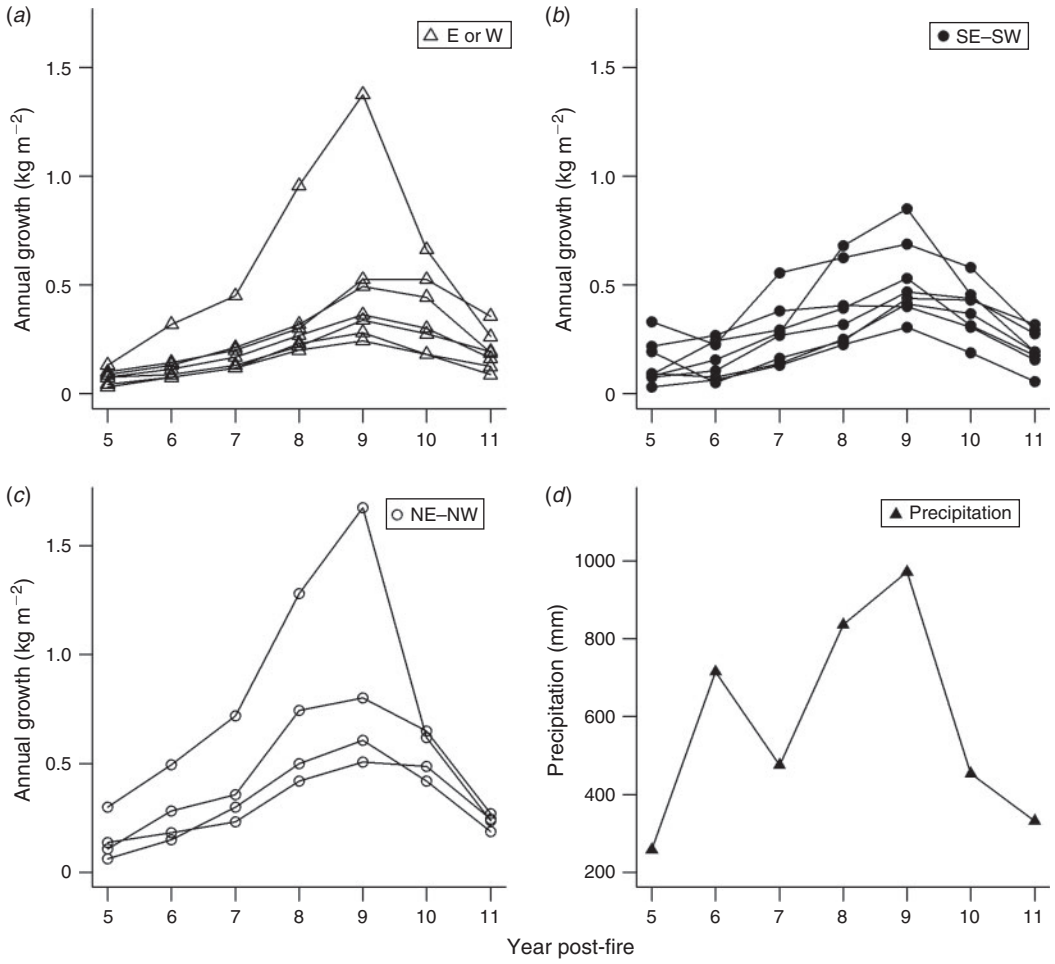

Fig. 2. Annual biomass increment in each year post-fire in plots facing (*a*) directly east or directly west; (*b*) south-east to south-west; and (*c*) north-east to north-west. Annual precipitation is shown in (*d*).

each year of growth is shown in Fig. S3*b*. Most plots show a peak that occurs at Year 9 (the growth that occurred during the 2010–11 growing season). This pattern persists when the differences in area are converted to differences in biomass, as shown in Fig. 2*a–c*. The biomass increment peak at Year 9 is aligned with the year of highest precipitation during the study period (Fig. 2*d*). A positive, significant correlation was found between annual precipitation and average annual biomass growth ($r = 0.75$, $P = 0.05$, $n = 7$). The relationship between biomass increment and age is non-linear, and there were insufficient data to disentangle the effect of precipitation from age-related trends.

Plot biomass estimates generated in this study, for the plots in which growth rings were available and *C. crassifolius* was the dominant species (15 total), varied by a factor of 3.5 from highest to lowest (Fig. 3). The range of values is consistent with those previously measured using a 21-year-old growth-ring reconstruction of 11 *C. crassifolius*-dominated plots (Riggan *et al.* 1988). The two datasets show very similar growth trajectories for their overlapping years since burning.

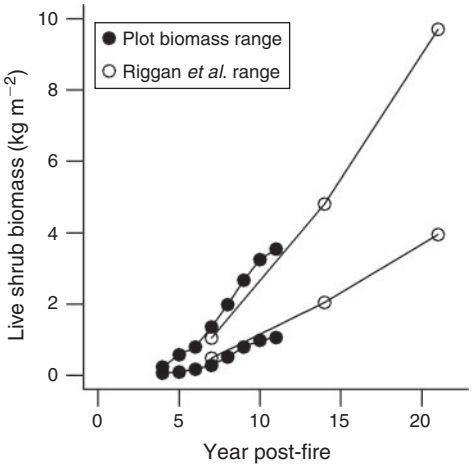

Fig. 3. Maximum and minimum annual biomass values in *Ceanothus crassifolius*-dominated plots from this study (Years 4 through 11 post-fire) and values reconstructed from growth-ring measurements of 21-year-old *C. crassifolius* plots from the same general study area in Riggan *et al.* (1988) (Years 7, 14 and 21 post-fire).

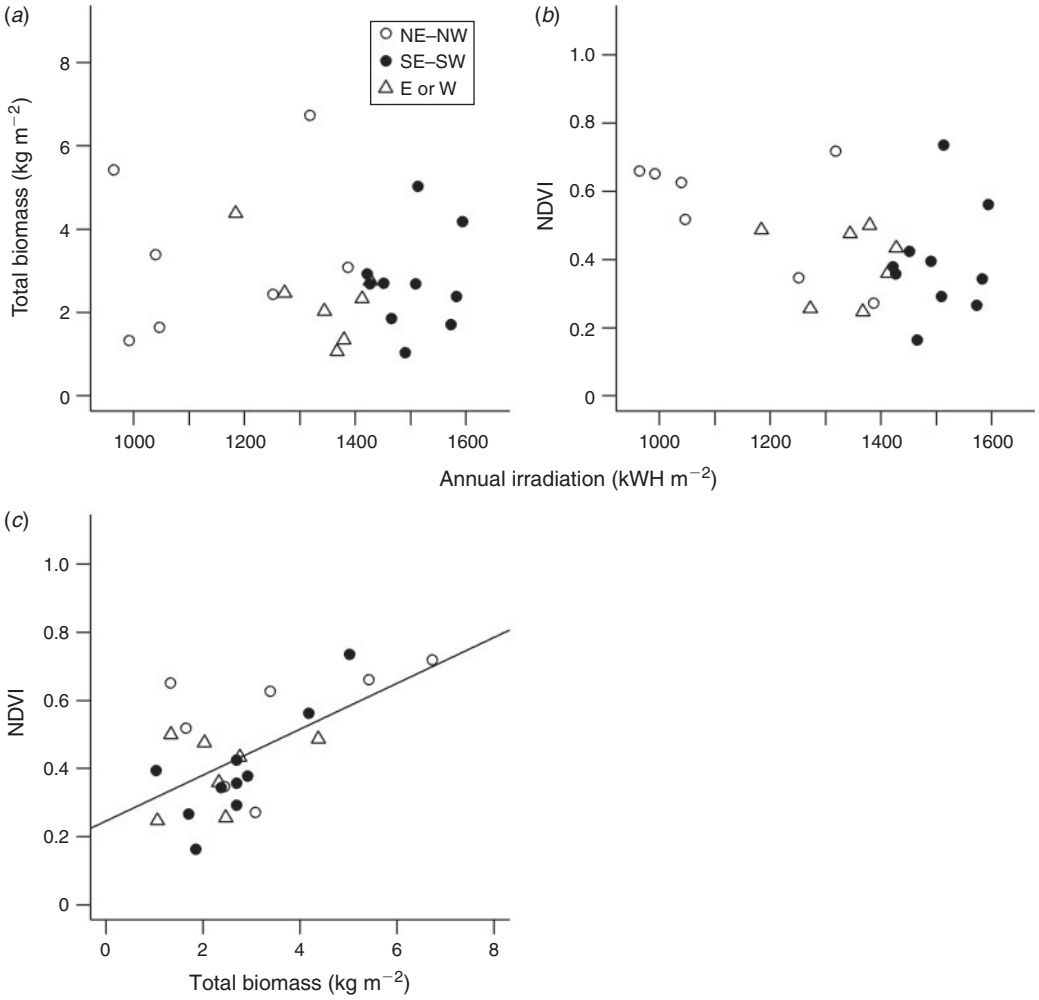

Fig. 4. (*a*) Total biomass and annual irradiation for each of the 24 field plots; (*b*) NDVI (Normalized Difference Vegetation Index) and annual irradiation; and (*c*) total biomass and NDVI. Plots are grouped into categories of north-east to north-west, south-east to south-west, and directly west- or east-facing.

Analysis of site characteristics

The irradiation analysis requires only the final biomass values, so we included the full set of 24 plots. No relationship between biomass and modelled irradiation is evident (Fig. 4*a*, $R^2 = 0.02$, $P = 0.6$, $n = 24$).

We calculated the average plot NDVI to serve as an independent verification of the pattern of irradiation and vegetation abundance. The regression of modelled annual irradiation and NDVI is not significant at the 0.01 significance level ($R^2 = 0.20$, $P = 0.03$, $n = 24$, Fig. 4*b*). However, the regression of total biomass and NDVI is significant ($R^2 = 0.37$, $P = 0.002$, $n = 24$, Fig. 4*c*).

Discussion and conclusion

Growth rings

We found that shrub growth rings provide a fairly straightforward and promising method to track patterns of biomass accumulation in the early years of post-fire recovery. Although most plots show a consistent overall temporal pattern of growth that tracked with the temporal variation of annual precipitation, there was considerable variation among plots (Fig. 3). Previous studies indicate that precipitation plays an important role in shaping the patterns of post-fire recovery (Keeley and Keeley 1981; Hope *et al.* 2007), and that the pattern of recovery is spatially variable (Kinoshita and Hogue 2011). Understanding the role of precipitation in shaping patterns of post-fire biomass accumulation is important, especially in light of higher temperatures and potential changes in precipitation magnitude and intensity in California that are expected with global climate change (Cayan *et al.* 2008; Pierce *et al.* 2013). If chaparral stands receive lower levels of precipitation for extended periods, they will likely recover more slowly after a fire (Prieto *et al.* 2009), although it is possible that increased water use efficiency due to higher levels of atmospheric CO_2 would compensate for this reduction in growth rate (Tague *et al.* 2009).

The annual growth plot shows a non-linear relationship with stand age, where growth peaks approximately 9 years following fire. In this particular study, precipitation also generally increased to a peak value for the first 9 years

following fire, so it is difficult to disentangle the effect of age from precipitation.

Although it is useful to convert the stem cross-sectional area to biomass, it requires the assumption that the regression equation relating biomass to stem area is consistent across years. Age-specific equations would provide a more accurate estimation of biomass, but we decided that for the purposes of this project, calculating biomass based on a single age would be sufficient.

Analysis of site characteristics

Cumulative irradiation has been shown in other studies of Mediterranean-type landscapes to be a useful predictor of biomass (Yool *et al.* 1985; Dahlin *et al.* 2012). It is unclear why no relationship was observed in the present study.

One possible explanation for the lack of statistical relationship with biomass is that there could be co-location errors between plot locations and the DEM from which irradiation values are derived. However, NDVI also shows little relationship with irradiation, and this was not dependent on any sort of field-based error. NDVI does exhibit a realistic relationship with measured biomass.

There are several other possible explanations for the lack of agreement in biomass and terrain-related variables. The spatial extent of the study area and number of plots might both be too small to detect a relationship. Analysis of terrain-related variables is commonly conducted over large spatial extents (e.g. Kopecký and Čížková 2010; Dahlin *et al.* 2012). Another possible factor might be that the study area is still in the early stages of post-fire recovery, and was not yet at a state of full canopy closure. Related to the matter of canopy closure development is the potential issue of plot size. We chose to use 16-m^2 plots because the smaller area was more tractable than the 64-m^2 plot size we had used in a previous chaparral study (Uyeda *et al.* 2015), especially considering the large number of plots. However, it is possible that plots 16 m^2 in area individually are too small to be representative of a given landscape element, particularly if canopy closure is incomplete.

Use of shrub growth rings is a promising technique for reconstructing stand development patterns of early post-fire chaparral, and would likely also work well in other Mediterranean-type shrublands. During the study period, precipitation had a significant role in shaping the annual patterns of biomass growth, and NDVI values based on high-spatial-resolution aerial imagery co-varied with field-based biomass values. Satellite-based NDVI time-series data are often used to understand patterns of biomass accumulation in shrublands at fairly coarse spatial resolutions (e.g. McMichael *et al.* 2004; Uyeda *et al.* 2015; Potter 2016). As shown in the current study, biomass levels can vary substantially over short distances, so relating coarse-resolution imagery to field-based measurements of biomass can be problematic. Imagery with high spatial resolution is not typically available at an annual temporal resolution, so plot-based growth-ring data provide important information on annual growth that would not otherwise be available.

In future work, we plan to examine the relation of patterns in biomass recovery, as measured here, to a time series of satellite-based metrics of vegetation growth. This will help to determine if metric relationships from satellite-based imagery provide a feasible way to scale field-intensive measures of shrub growth across larger areal extents.

Acknowledgements

Mike Oxford from the USDA Forest Service arranged for access to SDEF. I. Schmidt, Y. Granovskaya, J. McCullough, K. Walsh, A. Clark, J. Schichtel, L. Handa, M. Hartfelder, K. Hartfelder, E. Storey, R. Elliott and A. Lewis provided assistance with field vegetation sampling. J. Reichling and E. Reichling provided access to sanding equipment and workspace. Funding for this project was provided by the USDA Forest Service through American Recovery and Reinvestment Act Agreement no. 10-JV-11279701–10: 'Airborne remote sensing to enable hazardous fuels reduction, forest health protection, rehabilitation and hazard mitigation activities on Federal lands', Dr Philip Riggan, Principal Investigator.

References

Baldwin BG, Goldman DH, Keil DJ, Patterson R, Rosatti TJ, Wilken DH (2012) 'The Jepson manual: vascular plants of California.' (University of California Press: Berkeley, CA)

Black CH (1987) Biomass, nitrogen, and phosphorus accumulation over a southern California fire cycle chronosequence. In 'Plant response to stress – Functional analysis in Mediterranean ecosystems'. (Eds JD Tenhunen, FM Catarino, OL Lange, WC Oechel) pp. 445–458. (Springer: Berlin). doi:10.1007/978-3-642-70868-8_29

Bouriaud O, Bréda N, Dupouey J-L, Granier A (2005) Is ring width a reliable proxy for stem-biomass increment? A case study in European beech. *Canadian Journal of Forest Research* **35**, 2920–2933. doi:10.1139/X05-202

Cayan DR, Maurer EP, Dettinger MD, Tyree M, Hayhoe K (2008) Climate change scenarios for the California region. *Climatic Change* **87**(Suppl 1), 21–42. doi:10.1007/S10584-007-9377-6

Clark DA, Brown S, Kicklighter DW, Chambers JQ, Thomlinson JR, Ni J (2001) Measuring net primary production in forests: concepts and field methods. *Ecological Applications* **11**, 356–370. doi:10.1890/1051-0761(2001)011[0356:MNPPIF]2.0.CO;2

Coale TH, Deveny AJ, Fox LR (2011) Growth, fire history, and browsing recorded in wood rings of shrubs in a mild temperate climate. *Ecology* **92**, 1020–1026. doi:10.1890/10-1611.1

Dahlin KM, Asner GP, Field CB (2012) Environmental filtering and land-use history drive patterns in biomass accumulation in a Mediterranean-type landscape. *Ecological Applications* **22**, 104–118. doi:10.1890/11-1401.1

Duren OC, Muir PS (2010) Does fuels management accomplish restoration in south-west Oregon, USA, chaparral? Insights from age structure. *Fire Ecology* **6**, 76–96. doi:10.4996/FIREECOLOGY.0602076

Fritts HC, Swetnam TW (1989) Dendroecology: a tool for evaluating variations in past and present forest environments. *Advances in Ecological Research* **19**, 111–188. doi:10.1016/S0065-2504(08)60158-0

Hope A, Tague C, Clark R (2007) Characterizing post-fire vegetation recovery of California chaparral using TM/ETM+ time-series data. *International Journal of Remote Sensing* **28**, 1339–1354. doi:10.1080/01431160600908924

Husch B, Beers TW, John A, Kershaw J (2003) 'Forest mensuration.' (John Wiley & Sons, Inc.: Hoboken, NJ)

Jensen JR (2007) 'Remote sensing of the environment: an Earth resource perspective.' (Pearson Prentice Hall: Upper Saddle River, NJ)

Keeley JE (1993) Utility of growth rings in the age determination of chaparral shrubs. *Madrono* **40**, 1–14. Available at http://www.jstor.org/stable/41424935 [Verified 31 May 2016]

Keeley JE, Keeley SC (1981) Post-fire regeneration of southern California chaparral. *American Journal of Botany* **68**, 524–530. doi:10.2307/2443028

Kinoshita AM, Hogue TS (2011) Spatial and temporal controls on post-fire hydrologic recovery in southern California watersheds. *Catena* **87**, 240–252. doi:10.1016/J.CATENA.2011.06.005

Kopecký M, Čížková Š (2010) Using topographic wetness index in vegetation ecology: does the algorithm matter? *Applied Vegetation Science* **13**, 450–459. doi:10.1111/J.1654-109X.2010.01083.X

McMichael CE, Hope AS, Roberts DA, Anaya MR (2004) Post-fire recovery of leaf area index in California chaparral: a remote sensing-chronosequence approach. *International Journal of Remote Sensing* **25**, 4743–4760. doi:10.1080/01431160410001726067

Pasquini SC, Vourlitis GL (2010) Post-fire primary production and plant community dynamics in chaparral stands exposed to varying levels of nitrogen deposition. *Journal of Arid Environments* **74**, 310–314. doi:10.1016/J.JARIDENV.2009.08.013

Pierce DW, Cayan DR, Das T, Maurer EP, Miller NL, Bao Y, Kanamitsu M, Yoshimura K, Snyder MA, Sloan LC, Franco G, Tyree M (2013) The key role of heavy precipitation events in climate model disagreements of future annual precipitation changes in California. *Journal of Climate* **26**, 5879–5896. doi:10.1175/JCLI-D-12-00766.1

Potter CS (2016) Vegetation regrowth following wildfires in the Santa Cruz Mountains of northern California monitored using Landsat satellite image analysis. *Open Journal of Forestry* **6**, 82–93. doi:10.4236/OJF.2016.62008

Prieto P, Peñuelas J, Llusià J, Asensio D, Estiarte M (2009) Effects of experimental warming and drought on biomass accumulation in a Mediterranean shrubland. *Plant Ecology* **205**, 179–191. doi:10.1007/S11258-009-9608-1

Rich P, Dubayah RC, Hetrick W, Saving S (1994) Using viewshed models to calculate intercepted solar radiation: applications in ecology. American Society for Photogrammetry and Remote Sensing Technical Papers, pp. 524–529. Available at http://professorpaul.com/publications/rich_et_al_1994_asprs.pdf [Verified 31 May 2016]

Riggan PJ, Goode S, Jacks PM, Lockwood RN (1988) Interaction of fire and community development in chaparral of southern California. *Ecological Monographs* **58**, 155–176. doi:10.2307/2937023

Röder A, Hill J, Duguy B, Alloza JA, Vallejo R (2008) Using long time series of Landsat data to monitor fire events and post-fire dynamics and identify driving factors. A case study in the Ayora region (eastern Spain). *Remote Sensing of Environment* **112**, 259–273. doi:10.1016/J.RSE.2007.05.001

Schlesinger WH, Gill DS (1980) Biomass, production, and changes in the availability of light, water, and nutrients during the development of pure stands of the chaparral shrub, *Ceanothus megacarpus*, after fire. *Ecology* **61**, 781–789. doi:10.2307/1936748

Smith AM (2016) Population demographics of *Ceanothus verrucosus* at Cabrillo National Monument, San Diego, California. MS Thesis, San Diego State University, CA.

Stohlgren T, Parsons DDJ, Rundel PPW (1984) Population structure of *Adenostoma fasciculatum* in mature stands of chamise chaparral in the southern Sierra Nevada, California. *Oecologia* **64**, 87–91. doi:10.1007/BF00377549

Tague C, Seaby L, Hope A (2009) Modeling the ecohydrologic response of a Mediterranean type ecosystem to the combined impacts of projected climate change and altered fire frequencies. *Climatic Change* **93**, 137–155. doi:10.1007/S10584-008-9497-7

Uyeda KA, Stow DA, Riggan PJ (2015) Tracking MODIS NDVI time series to estimate fuel accumulation. *Remote Sensing Letters* **6**, 587–596. doi:10.1080/2150704X.2015.1063736

Uyeda KA, Stow DA, O'Leary JF, Schmidt IT, Riggan PJ (2016) Spatial variation of fuel loading within varying-aged stands of chaparral. *Applied Vegetation Science* **19**, 267–279. doi:10.1111/AVSC.12209

Yool S, Eckhardt D, Estes J, Cosentino M (1985) Describing the brushfire hazard in southern California. *Annals of the Association of American Geographers* **75**, 417–430. doi:10.1111/J.1467-8306.1985.TB00076.X

Zammit C, Zedler P (1993) Size structure and seed production in even-aged populations of *Ceanothus greggii* in mixed chaparral. *Journal of Ecology* **81**, 499–511. doi:10.2307/2261528